Transition metal chalcogenides/graphene ensembles for light-induced energy applications

Antonia Kagkoura,[a] Theodosis Skaltsas[a] and Nikos Tagmatarchis*[a]

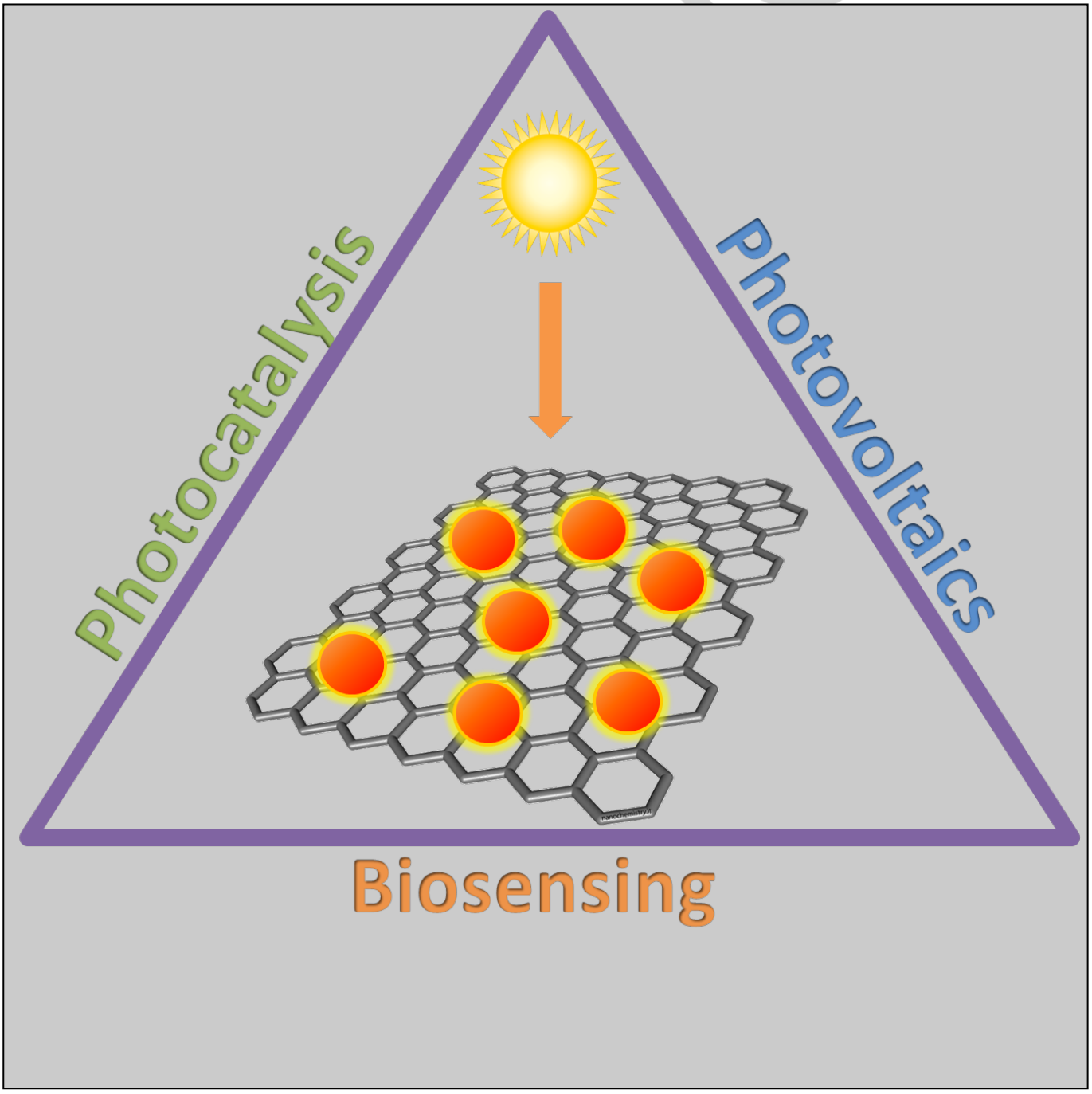

Abstract: Recently, nanomaterials that harvest solar energy and convert it to other forms of energy are of great interest. In this context, transition metal chalcogenides (TMCs) are lately on the spotlight due to their optoelectronic properties that render them potential candidates mainly in energy conversion applications. Integration of TMCs onto a strong electron accepting material, such as graphene, yielding novel TMC/graphene ensembles is of high significance, since photoinduced charge-transfer phenomena leading to intra-ensemble charge-separation, may occur. In this review, we highlight the utility of TMCs/graphene ensembles, with a specific focus on latest trends in applications, while their synthetic routes are also discussed. Precisely, TMC/graphene ensembles are photocatalytically active and superior as compared to intact TMCs analogues, when examined toward photocatalytic H_2 evolution, dye degradation and redox transformations of organic compounds. Moreover, TMC/graphene ensembles have shown excellent prospect when employed in photovoltaics and biosensing applications. Finally, the future prospects of such materials are outlined.

1. Introduction

The scientific interest for nanocrystals, also known as quantum dots, is continuously increasing, especially during the last decade, attracting more and more researchers to explore new synthesis methods and fully examine their structure and properties. Notably, such inorganic nanoparticles possess unique size-dependent physicochemical properties. Particularly, transition metal chalcogenides (TMCs) quantum dots, composed of a transition metal cation bonded with one or two chalcogenide anions (S, Se, Te), are of great interest[1-3] due to their semiconducting characteristics, absorption and emission of visible light.[4] The utility of TMCs in a variety of applications relies on diverse factors including their optoelectronic properties, size, shape, facets and surface area. In turn, these parameters mostly depend on reaction conditions employed during synthesis of TMCs, such as for example temperature, concentration, time and precursor materials utilized. Markedly, the quantum confinement effect, in other words the dependence of energy band-gap with the size of TMCs, gives rise to materials with tunable emission properties,[5] potentially suitable for solar light harvesting applications[6] and electrochemical applications.[7, 8] However, in photoexcited TMCs ultrafast recombination of the photo-generated electron and hole species occurs, resulting to low light conversion efficiency.[9] Hence, in order to overcome this hurdle, integration of TMCs to strong electron-accepting materials such as carbon nanostructures[10-13], i.e carbon nanotubes or graphene. In particular, the inherent novel properties of graphene, such as conductivity and ballistic charge-transport, are beneficial for targeting energy applications.

Graphene is a single atomic plane of sp^2 hybridized carbon atoms arranged in a two-dimensional honeycomb lattice,[14-16] potentially suitable for a vast number of applications spanning from materials to life science. Specifically, due to its novel and outstanding conducting and electronic properties (quantum Hall effect, electrical conductivity ≈ 6000 S cm^{-1}, ideal electron mobility ≈ 200 000 cm^2 V^{-1} s^{-1}),[14, 17, 18] graphene is set to take its

[a] A. Kagkoura, Dr. T. Skaltsas and Dr. N. Tagmatarchis
Theoretical and Physical Chemistry Institute
National Hellenic Research Foundation
Vassileos Constantinou Avenue, Athens 11635, Greece
E-mail: tagmatar@eie.gr

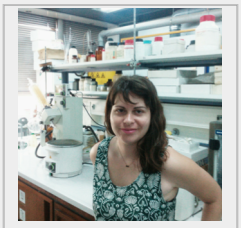

Antonia Kagkoura received her bachelor degree in Materials Science from the University of Patras in Greece. She continued her studies with a master's degree at the University of Edinburgh, Scotland. She is currently a Marie-Curie early-stage researcher at the Theoretical and Physical Chemistry Institute, National Hellenic Research Foundation in Athens, Greece, en route to PhD under the supervision of Dr. Nikos Tagmatarchis. Her research interests focus on the synthesis and characterization of carbon-based hybrid materials with semiconductor nanoparticles as well as their applications.

Theodosis Skaltsas is post-doctoral researcher in Theoretical and Physical Chemistry Institute, at the National Hellenic Research Foundation, in Athens, Greece. He received his Ph.D in this institute, under the supervision of Dr. N. Tagmatarachis in 2016. His research interests include functionalization of carbon nanostructrures with polymers and/or semiconducting nanoparticles, aiming to energy conversion applications.

Nikos Tagmatarchis is Deputy Director and Member of the Scientific Council of the Theoretical and Physical Chemistry Institute, at the National Hellenic Research Foundation, in Athens, Greece. His research interests focus in the chemistry of carbon-based nanostructured materials, particularly in the context of charge-transfer and catalytic processes for energy applications. He has been recipient of the European Young Investigator Award (2004), Visiting Professor at the Chinese Academy of Sciences (2011-2012) and Invited Fellow by the Japan Society for the Promotion of Science (2013-2014).

place alongside semiconductors in electronic devices.[16]

In principle, inorganic nanoparticles can either be directly immobilized onto the surface of graphene sheets or alternatively grown, depending on the nature of graphene employed, i.e. graphene oxide (GO), reduced graphene oxide (RGO), exfoliated graphene (EG). For example, on a GO substrate that contains a plethora of oxygen-based functionalities where seeding can occur, growth of nanoparticles is considered easier. In contrast, on EG that lacks defected sites for direct interactions, deposition of previously grown nanoparticles is the route for choice. Toward this direction, numerous transition metals have been utilized by employing diverse synthetic protocols for the preparation of semiconducting TMC-based nanoparticles incorporating cadmium,[19] zinc,[20] copper,[21] or molybdenum[22]. Due to efficient electron transfer phenomena that occur from semiconducting TMCs to graphene, such hybrid species are considered as efficient materials en route to energy conversion applications, particularly for the photocatalytic water purification and hydrogen production.[23, 24]

Amongst the routes employed for the preparation of TMCs/graphene ensembles, deposition of TMCs onto graphene sheets via a solvothermal process is the most widely applied strategy. Additionally, traditional chemical deposition methods, electrochemical, ultrasonication as well as laser synthesis deposition have been also considered. In this review, we present the latest research trend in TMCs/graphene ensembles, focusing on TMCs based on VIA, IB and IIB metals of the periodic table. Furthermore, in an attempt to classify our work, the hybrid materials are categorized according to targeted application. Initially, the photocatalytic performance of TMCs/graphene nanoensembles toward (a) hydrogen evolution, (b) organic dyes degradation, and (c) redox transformations are examined, then the incorporation of graphene/TMCs onto photovoltaic devices is surveyed, and ultimately the review focuses on the prospects these hybrid materials show as photodetectors and biosensors.

2. TMCs/Graphene Ensembles for Photocatalysis

2.1. Hydrogen evolution

Sustainable hydrogen production, particularly from water splitting, as a clean and renewable fuel, is a major challenge and therefore, advanced photocatalytic systems that result in increased efficiency for the hydrogen evolution reaction (HER) are of significant importance.[25, 26] The most widely applied catalyst for the HER, owed to its effectiveness, is Pt-based metals. However, Pt is expensive, hence, it is of particular interest and challenging the development of highly active HER catalysts based on abundantly produced and inexpensive materials. New replacement materials as catalysts for the HER should be reasonably stable and show high production rates for hydrogen, while absorbing in the visible region in order to exploit as much higher solar energy as possible. Toward this direction, significant research effort has been devoted to the development of novel hybrid materials, in which the outstanding properties of graphene are combined with those of TMCs, as potential photocatalysts for hydrogen production from water splitting.

A widely used method to prepare CdS/graphene hybrids concerns the *in-situ* solvothermal route, in which graphene as support, a cadmium precursor (e.g. cadmium acetate) and a sulfur precursor[27-29] [e.g. dimethyl sulfoxide (DMSO) which could also serve as solvent] are introduced in an autoclave reactor and heated. According to this process, CdS/GO ensembles exhibiting high efficiency in the photocatalytic hydrogen evolution under visible light irradiation were effectively prepared.[30] Notably, the presence of GO as part of the hybrid material enhances the crystallinity and the specific surface area of CdS, since only a small amount of GO can dramatically improve the photocatalytic activity of the system. The incorporation of GO resulted in the highest visible-light photocatalytic H_2-production rate reported so far for TMCs/graphene photocatalysts, although this value was achieved with the incorporation of platinum as cocatalyst, which was approximately five times higher than that of bare CdS nanoparticles. Interestingly, the photocatalytic activity is rather attributed to the increased specific surface area of the hybrid material and to a less extent to the electron accepting property of graphene. Similarly, materials comprised of sulfonated graphene and CdS nanoparticles were fabricated by a one-pot solution method, demonstrating the utility of graphene as a cheap co-catalyst to boost the photocatalytic hydrogen production from water.[31] The formation of CdS nanoparticles onto the active sites of sulfonated graphene was triggered by the introduction of a cadmium precursor, while their growth is owed to the sulfur precursor (i.e. Na_2S). Markedly, highly efficient generation of hydrogen was demonstrated in the presence of a sacrificial reagent that is actually comparable to systems containing Pt as co-catalyst. Mechanistically, the photogenerated electrons formed after the dissociation of excitons at the interface of CdS/graphene are successfully transported with negligible loss of energy onto the surface of graphene and effectively employed to split water and generate hydrogen, according to Scheme 1. Moreover, the presence of graphene is beneficial for enhancing the hydrogen production because not only reduces the charge recombination rate but also aids the distribution of the nanoparticles onto the graphitic lattice, creating in this way more photocatalytically active sites and increased surface area. All these characteristics are favorable for improved HER performance.

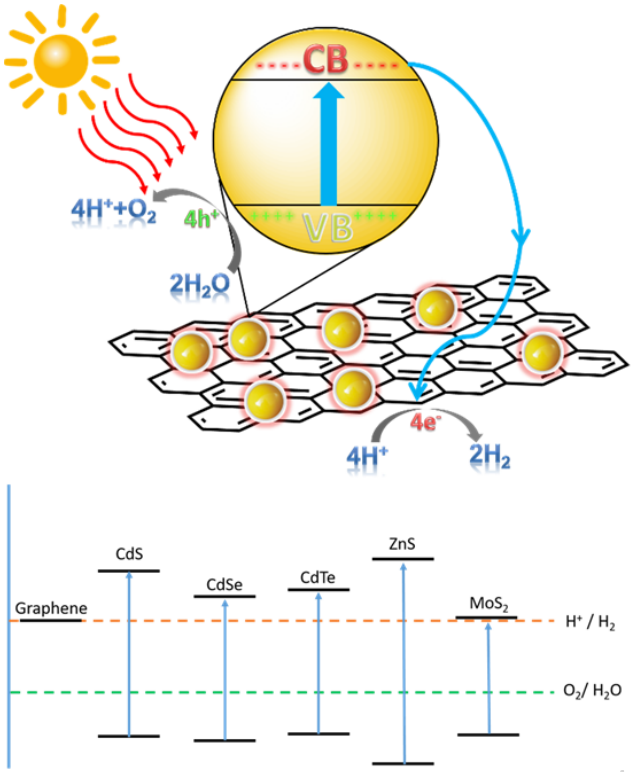

Scheme 1. Upper panel: Electron-transfer and charge-separation occurring within a quantum dot/graphene hybrid material upon light irradiation. Photoexcited electrons in the semiconducting quantum dots are transferred to electron-accepting graphene and transported along the sheets, triggering water splitting and hydrogen evolution. Lower panel: Relative energy levels of some chalcogenides and graphene, compared with water splitting potentials.

Meanwhile, similar synthetic routes were employed for the fabrication of ensembles incorporating nitrogen-doped graphene and CdS nanoparticles, abbreviated as CdS/N-graphene.[32] The N-graphene was prepared by annealing of GO in the presence of gaseous ammonia, while the CdS/N-graphene ensembles were developed by exploiting the active sites of N-graphene towards the formation of CdS nanoparticles by employing the appropriate cadmium and sulfur precursors. Similarly with previous cases, CdS/N-graphene showed about 5 times higher photocatalytic activity for hydrogen evolution under visible light irradiation as compared to intact CdS. Furthermore, significant results were observed when the photocatalyst was recycled and tested for more than 30 hours of irradiation, without losing efficiency, which is of high importance when aiming to industrial applications. The high efficiency was attributed to intra-ensemble electron-transfer phenomena from CdS to N-doped graphene and the reduced electron-hole recombination rate, which were identified with the aid of transient photocurrent assays and by the enhanced photoresponse revealed for CdS/N-graphene as compared to the bare CdS. Furthermore, the efficiency of CdS/N-graphene hybrids was found superior when compared with that of graphene and GO analogous hybrids, which is attributed to the enhanced conductive character of N-graphene after the nitrogen doping. Moreover, N-graphene acts as a protective layer to CdS, hence, highlighting in this way the remarkable high resistance of the nanoensemble as catalyst against photocorrosion.

Except from the aforementioned and analyzed *in-situ* approaches, graphene/CdS ensembles were also fabricated by simple mixing of the two components. According to this, stable aqueous dispersions of polymer-modified graphene sheets were prepared via the *in-situ* reduction of GO in the presence of cationic poly(allylamine hydrochloride).[33] In such a way, well-defined CdS/graphene films were fabricated via self-assembly from the tailor-made negatively charged CdS and the positively charged graphene sheets decorated with the cationic poly(allylamine hydrochloride), according to Scheme 2. This alternative stacking manner, the incorporation of CdS within graphene by layer-by-layer technique, leads to the maximization of charge-separation. As a result, the photoelectrochemical and photocatalytic performance of CdS/graphene films under visible light irradiation were observed at least two times improved, in comparison with that of neat CdS nanoparticles.

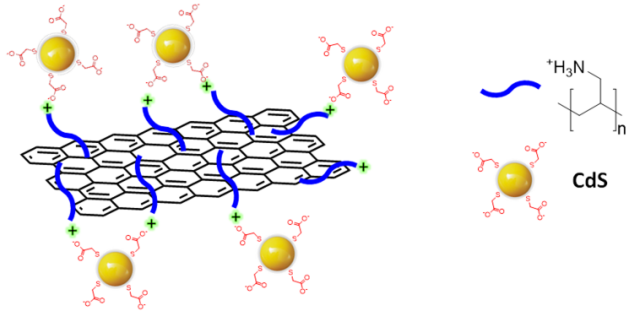

Scheme 2. Schematic illustration for the CdS/graphene ensemble as formed upon attractive electrostatic interactions of positively charged graphene/poly(allylamine hydrochloride) with CdS nanoparticles carrying negative charges owed to thioglycolic acid stabilizer.

Furthermore, by exploiting the carboxyl groups of the amphiphilic block copolymer poly(isoprene-*b*-acrylic acid) (PI-*b*-PAA) which was used as stabilizer to grow CdS nanoparticles, aqueous dispersions of CdS•PI-*b*-PAA/graphene ensembles were prepared (Scheme 3). Briefly, the hydrophobic poly(isoprene) block of the copolymer, interacted non-covalently with exfoliated graphene. Following that, the cadmium precursor was introduced into the system, where the cadmium cations interacted with the negatively charged carboxylic groups of the poly(acrylic acid) block. At the last stage, upon introduction of the sulfur precursor, *in-situ* formation of CdS nanoparticles onto graphene/PI-*b*-PAA was achieved. The complementary characterization of the material gave clear evidence of charge transfer phenomena between the semiconducting CdS and graphene and subsequently its photocatalytic performance was scrutinized.[34] Specifically, the photocatalytic activity of CdS•PI-*b*-PAA/graphene was tested for hydrogen generation from water splitting, by examining the reduction of 4-nitroaniline to *p*-phenylenediamine. The production of hydrogen by water splitting aided by the photocatalytic presence of CdS•PI-*b*-PAA/graphene was confirmed by observing changes in the absorption spectrum

of 4-nitroaniline upon short time intervals of visible light irradiation. Notably, the formation of *p*-phenylenediamine was approximately 10 times faster and much more efficient in the presence of CdS•PI-*b*-PAA/graphene as a photocatalyst, compared to the reference CdS•PI-*b*-PAA, where graphene was absent. Mechanistically, photoexcitation of CdS under visible illumination, creates hole-electron pairs; in the presence of graphene, the photogenerated electrons are accumulated and transported onto the graphene sheets, while in absence of graphene the charge recombination of hole-electron is an ultrafast process. On the other hand, the photogenerated holes are quenched in the presence of a sacrificial agent such as ammonium formate. The accumulated electrons on graphene are used to reduce water resulting on the evolution of hydrogen as demonstrated by the reduction of 4-nitroaniline to *p*-phenylenediamine.

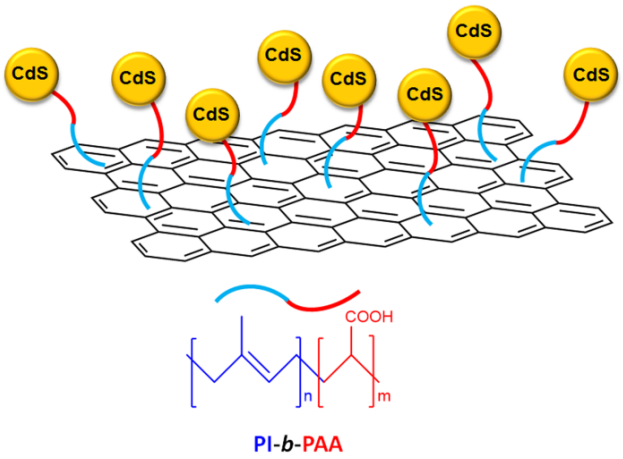

Scheme 3. Schematic illustration for the CdS•PI-*b*-PAA/graphene nanoensemble. The poly(isoprene) block of the copolymer interacts with exfoliated graphene via hydrophobic van der Waals forces, while the poly(acrylic acid) block acts as a stabilizer for the formation of CdS nanoparticles.

Considering the toxic nature of cadmium the scientific interest was moved to more sophisticated systems in which the amount of cadmium was partially or completely replaced by other metals. Hence, ZnS/graphene/MoS_2 hybrids were constructed and examined toward their efficiency for the production of hydrogen. The ZnS nanoparticles were easily prepared by following a hydrothermal method, in the presence of the two-dimensional heterostructure graphene/MoS_2. Notably, the presence of MoS_2 as co-catalyst in ZnS nanoparticles loaded onto graphene resulted on the highest photocatalytic rate of hydrogen evolution so far for TMCs/graphene materials, without the introduction of precious metals, such as platinum, as well as good recurrence stability.[35] The enhanced performance of ZnS/graphene/MoS_2 is owed to the cooperative effect of graphene and MoS_2 as co-catalysts, opening wide avenues toward the realization of novel materials for the HER without requiring the presence of any noble metals.

Even more complex systems composed of ternary quantum dots, consisting of two different transition metals and a chalcogen atom combined with graphene sheets were developed and tested. For example, the noble metal-free RGO-$Zn_xCd_{1-x}S$ nanoensemble fabricated by a facile co-precipitation-hydrothermal reduction route and the $Zn_xCd_{1-x}S$-graphene realized by a one-step hydrothermal method by employing zinc, cadmium and a sulfur precursor, was found to exhibit good photocatalytic activity, although their H_2 production rate was comparable with CdS/graphene hybrids.[27, 28] Interestingly, $Zn_{0.8}Cd_{0.2}S$-RGO hybrid material exhibited the highest quantum efficiency (23.4%) ever reported among TMC/graphene ensembles employed for the photocatalytic hydrogen production.

Although two-dimensional heterostructures combining MoS_2 and WS_2 nanoflakes onto graphene have been described, the decoration of graphene sheets with MoS_2 nanoparticles is scarce. To the best of our knowledge, there is only a single report dealing with the synthesis of MoS_2 nanoparticles on RGO. Briefly, MoS_2/RGO was acquired via a one-step solvothermal reaction of $(NH_4)_2MoS_4$ and hydrazine in a solution of mildly oxidized graphene sheets. Interestingly, the particular MoS_2/RGO exhibits superior electrocatalytic activity in the HER as compared to other MoS_2 catalysts.[36] The remarkable performance of MoS_2/RGO is attributed to the plenty catalytic edge sites that are present on the MoS_2 nanoparticles and the excellent electrical coupling of MoS_2 with the graphene network, within the MoS_2/RGO ensemble. In another example, a hybrid material consisting of TiO_2 nanocrystals was grown in the presence of a layered MoS_2/graphene and the high photocatalytic HER performance was attributed to MoS_2 and graphene's synergistic effect, where the two components efficiently suppress charge recombination, thereby improving interfacial charge transfer as well as creating a greater number of active adsorption sites and photocatalytic reaction centers.[37] More precisely, the incorporation of graphene to TiO_2, resulted to 7 times higher hydrogen production rate, whereas the TiO_2/MoS_2/graphene hybrid showed approximately 40 times increased hydrogen production rate, compared to the main photocatalytically active material, i.e TiO_2.

As far as transition metal chalcogenides incorporating selenides concern, $MoSe_2$/RGO ensembles were prepared via a hydrothermal method with the introduction of the precursors in the presence of GO followed by low temperature annealing.[38] Comparison between MoS_2 and $MoSe_2$ revealed that the onset potentials of $MoSe_2$ and $MoSe_2$/RGO are significantly lower than those of MoS_2 and its graphene hybrids, highlighting the improved HER activity of $MoSe_2$ as compared to MoS_2. Moreover, density functional theory calculations revealed that the Gibbs free energy for atomic hydrogen adsorption on the $MoSe_2$ edges was closer to thermoneutral than that of MoS_2, thus, further confirming that $MoSe_2$ nanosheets are potentially better catalysts than the corresponding MoS_2 ones.

In order to better evaluate the photocatalytic activity of the currently reviewed TMC/graphene ensembles, the data concerning the hydrogen production rate and quantum efficiency

are summarized and presented in Table 1. For the cadmium-based chalcogenides with graphene, the highest H_2-production rate was reported for the CdS/GO material.[30] In fact the latter displays the highest reported H_2-production under light illumination for TMC/graphene ensembles, which is ascribed to the significantly improved crystallinity and specific surface area of CdS by the introduction of GO. Markedly, Pt was employed as cocatalyst, boosting itself the photocatalytic performance of CdS/GO as compared to the cases where only CdS/graphene and CdS/N-

Table 1. Photocatalytic performance of the reviewed TMC/graphene ensembles in terms of hydrogen production rate and quantum efficiency.

Material	H_2-production rate (mmol $h^{-1}g^{-1}$)	Cocatalyst content	Quantum efficiency %	Optimum graphene content wt %	Ref.
CdS/GO/Pt	55.720	0.5 wt% Pt	22.5	1	30
CdS/graphene	0.167	-	-	2	31
CdS/N-doped graphene	1.050	-	-	2	32
CdS/graphene	0.495				
ZnS/graphene/MoS_2	2.258	2 wt% MoS_2	-	0.25	35
ZnS/graphene	1.688				
$Zn_{0.8}Cd_{0.2}S$/RGO	1.824	-	23.4	0.25	27
$Zn_{0.5}Cd_{0.5}S$/graphene	1.060	-	19.8	0.5	28
TiO_2/MoS_2/graphene	2.060	0.5 wt% MoS_2	9.7	0.25	37

graphene were examined and exhibited lower H_2-production rates.[31, 32] It should be noted that when sulfonated graphene was employed, the hydrogen production yield of the CdS/graphene ensemble[31] was lower as compared to the case where RGO was used,[32] suggesting that conductivity is higher in the latter as attributed to the restoration of the sp^2 network, while in the former the presence of sp^3 sites decreases electronic transportation. The hydrogen production was enhanced upon replacing the Cd with Zn in the TMC/graphene ensembles,[27, 28] while also the presence of MoS_2 as cocatalyst further improves the photocatalytic process.[35, 37] Evidently, future assays employing MoS_2 not only as cocatalyst within TMC/graphene ensembles for the photocatalytic hydrogen production but also as stand-alone material for replacing graphene.

2.2. Dye degradation

Organic dyes are nowadays used extensively from industry for numerous applications resulting to huge amounts of organic waste that often leads to sea, rivers and groundwater contamination. In most cases these organic contaminants are water soluble making their removal from water impossible with conventional methods such as filtration and centrifugation. Moreover, other approaches such as adsorption on activated carbon, ultrafiltration, reverse osmosis, coagulation by chemical agents, ion exchange on synthetic adsorbent resins, although can be used efficiently, yet they are non-destructive, since they just transfer organic molecules from water to another phase, thus causing secondary pollution.[39] For this reason, various advanced oxidation processes have been established. Among these, photocatalysis in presence of semiconducting materials in aqueous phase causes the creation of highly reactive species, such as hydroxyl radicals that promote the oxidation of these organic pollutants. Titanium oxide in several forms has already been thoroughly employed toward this direction with effective results.[40-42] However, one of the biggest drawbacks is that TiO_2 absorbs light only in the UV-region. Consequently, TMCs absorbing in the visible region are considered as better photocatalyst candidates.[43-45] Moreover, their integration onto graphene sheets is beneficial since graphene acts as an electron acceptor, thus inhibiting the fast electron-hole recombination, resulting to enhanced photocatalytic activity. The advantageous profile of graphene is further justified by considering its large surface area and pore volume together with its large-scale production and relatively low-cost availability.

In this fashion, aqueous dispersions of CdS•PI-*b*-PAA/graphene ensembles that were analyzed above for their enhanced photocatalytic performance in hydrogen production,[34] were also exploited to degrade the water pollutant Rhodamine B (RhB). Particularly, when CdS•PI-*b*-PAA/graphene was used as photocatalyst the kinetics were much faster under visible light irradiation in the presence of air, than CdS•PI-*b*-PAA or neat exfoliated graphene. Charge transfer phenomena were identified between CdS and graphene, by observing the efficient quenching of the characteristic emission owed to CdS. Hence, it

is deduced that graphene acts as an efficient electron acceptor, facilitating charge separation. Then, the accumulated electrons on graphene react with molecular oxygen and create highly reactive radicals, such as HOO• and HO•, which in turn attack and degrade RhB, according to Scheme 4.

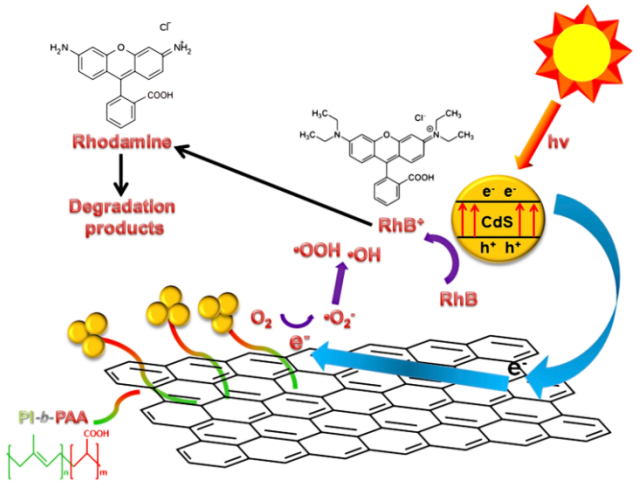

Scheme 4. Illustration of the photocatalytic RhB degradation mechanism owed to electron-transfer processes that occur within the CdS•PI-*b*-PAA/graphene ensemble.

Similarly, CdS/graphene ensembles were prepared following a simple precipitation reaction between Cd^{2+} ions and thiourea in the presence of GO and poly(vinylpyrrolidone) in ethylene glycol.[46] According to that process, CdS nanospheres were uniformly scattered on graphene sheets nicely evidenced by TEM imaging, while photoluminescence assays revealed the successful transfer of photoexcited electrons from CdS to graphene sheets. Moreover, CdS/graphene exhibited remarkable activity and stability toward the visible light driven degradation of RhB as substantiated by UV-Vis spectroscopy. Notably, the CdS/graphene catalyst can be recovered and reused for a number of subsequent catalytic cycles without losing efficiency.

Ternary TMCs combined with graphene have been also reported for the dye degradation processes. According to this, $Zn_{0.5}Cd_{0.5}S$/RGO was synthesized via the conventional *in-situ* co-precipitation-hydrothermal method and employed for degradation of Reactive Black 5 (RB5), under a low-power energy-saving daylight bulb at ambient conditions.[29] The authors also suggested a plausible mechanism towards the photocatalytic RB5 degradation. This was realized by introducing various h^+, $HO^•$ or $O_2^{•-}$ scavengers, such as *tert*-butanol (•OH scavenger), isopropanol ($HO^•$ scavenger), triethanolamine (h^+ scavenger), benzoquinone ($O_2^{•-}$ scavenger) and N_2 purging ($O_2^{•-}$ scavenger), showing in this way that these highly reactive species are responsible for the degradation process.

Although volatile metal (i.e. Zn, Cd) chalcogenides were extensively tested for the photocatalytic dye degradation, TMCs composed of other metals, such as copper were also examined. For example, CuS/RGO was prepared following an one-step, sonochemical route, upon which thioacetamide as reducing agent was mixed with a dispersion of $CuCl_2$ and GO in ethylene glycol.[47] The CuS/RGO exhibited high photocatalytic activity toward the degradation of methylene blue as compared to bare CuS, as rationalized by the enhanced light absorption of CuS, the strong dye absorption and the efficient charge-transport in RGO within CuS/RGO.

In an attempt to investigate further the photocatalytic dye degradation assisted by graphene-based catalysts, transition metal selenides have been also employed. Undoubtedly the presence of graphene is beneficial for improved photocatalytic performance as compared to bare TMCs. In this context, ZnSe/N-doped graphene was fabricated via a facile, catalyst free, one pot hydrothermal method at low temperature using RGO nanosheets and ZnSe(diethylenetriamine)$_{0.5}$ nanobelts as precursors (abbreviated as ZnSe(DETA)$_{0.5}$).[48] The ZnSe(DETA)$_{0.5}$ was used not only as the origin for the ZnSe nanorods but also as the nitrogen source for the graphene doping, while the ZnSe was deposited on the surface of graphene. These hybrids exhibited enhanced electrochemical performance for oxygen reduction reaction, as well as enhanced photocatalytic activities for the bleaching of methyl orange dye under visible-light irradiation, as compared to bare ZnSe.

2.3. Photoredox Activity

Beyond the photocatalytic hydrogen evolution and dye degradation, TMCs/graphene has been employed as photocatalyst for selective transformation of organic compounds, such as for example the oxidation of alcohols. Again, the driving force for the oxidation of alcohols to the corresponding carboxylic acids is the photoinduced charge-separation that takes place within the TMCs/graphene ensemble. Recently, CdS nanoparticles were combined with two different types of graphene, namely GO and acid-treated-graphene (GOA).[49] In the latter, the GO sheets that were cut into smaller parts exhibited elevated colloidal stability, possessed higher amount of oxygenated functional groups as a result of the ultrasonic treatment of GO with acid. Moreover, the GOA exhibited enhanced electrical conductivity compared to conventional GO. Next, CdS-GO and CdS-GOA were obtained after the incorporation of CdS on the graphene sheets via a one-pot solvothermal method in dimethyl sulfoxide, with the latter exhibiting much higher photocatalytic activity toward the oxidation of benzyl alcohol to benzaldehyde and the reduction of the 4-nitroaniline to *p*-phenylenediamine. Interestingly, the controllable tailoring of the GO physicochemical characteristics, such as size, shape, morphology and density of oxygenated functional groups or colloidal stability resulted to increased electrical conductivity, compared to non-acid-treated GO, which in turn led to improved photoelectrochemical and photocatalytic behavior of these hybrid materials.

Markedly, a totally different photocatalytic mechanism, in which RGO in ZnS/RGO acts as an organic dye-like macromolecular “photosensitizer” for ZnS, instead of an electron acceptor was proposed.[50] According to this, the conventional hydrothermal protocol was followed for the *in-situ* growth of ZnS nanoparticles on the 2D platform of a GO sheet. In brief, Zn cations, originating from zinc chloride were attracted by the negative charges of GO, and subsequently the introduction of NaS_2 led to ZnS formation. The subsequent reduction of GO to RGO promotes the improved conductivity as compared to the starting insulating GO, while also provides better interfacial contact between ZnS nanoparticles and RGO. The

aforementioned ensembles showed visible light photoactivity toward aerobic selective oxidation of alcohols and epoxidation of alkenes under ambient conditions. Likewise, a series of CdS/graphene ensembles with different loadings of graphene were prepared and used as visible light photocatalysts for selective organic transformation.[51] By following a solvothermal approach, with the simultaneous formation of the CdS nanoparticles and the reduction of GO, the hybrid materials were successfully tested as visible light harvesting photocatalysts for the selective oxidation of alcohols to the corresponding aldehydes under mild conditions. The enhanced photocatalytic activity of the nanohybrids is owed to the high light absorption of the CdS and the improved electron conductivity of graphene as compared to GO.

Moving a step beyond, the addition of a third component on TMC/graphene results to enhanced performance and functionality.[52] The CdS/graphene/TiO_2 ternary hybrid material was fabricated by first stabilizing the CdS nanoparticles via an *in-situ* strategy onto GO with the aid of DMSO, and subsequently incorporating TiO_2 nanoparticles which led to the enhanced photocatalytic performance. The mechanism that triggers the oxidation of the alcohols to the corresponding aldehydes is identical with the one of the photocatalytic dye degradation processes, namely, the photogeneration of superoxide radicals that eventually induces oxidation (Scheme 5).

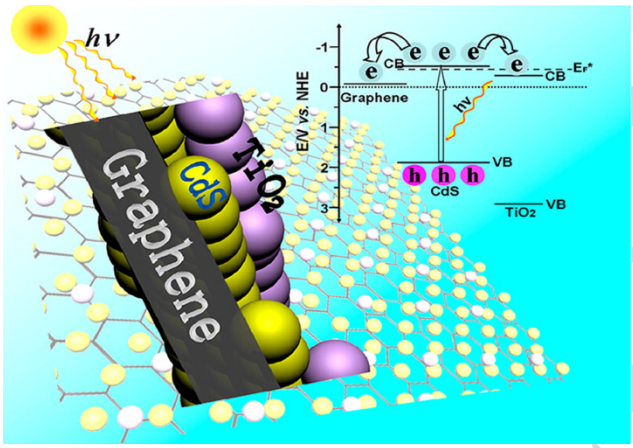

Scheme 5. Illustrative function of a CdS/graphene/TiO_2 ternary hybrid material as photocatalyst for the oxidation of alcohols to the corresponding aldehydes. Reprinted with permission from Ref. 52. Copyright 2012 American Chemical Society.

Finally, it was demonstrated that a CdS-RGO hybrid material shown better photocatalytic performance for the reduction of Cr(VI) as compared with that based on bare CdS nanoparticles.[53] Briefly, CdS-RGO hybrid materials were prepared by a one-step method, by introducing Cd and S precursors, along with GO, into a microwave reactor. Carboxylic acid groups of GO acted as anchoring sites, aiding the *in-situ* formation and growth of CdS nanoparticle, resulting to the reduction of GO to RGO and therefore to the fabrication of the hybrid material. The enhanced photocatalytic performance of CdS-RGO is attributed to both the increased light absorption intensity and the reduction of photoelectron-hole pair recombination in CdS upon the incorporation of RGO.

3. TMCs/Graphene Ensembles for Photovoltaics

Solar energy is a viable alternative to the fossil fuels energy sources, with the major advantage being that it is inexpensive and in principle endless. Hybrid materials composed of graphene and transition metal chalcogenides have been successfully tested for photovoltaic applications, photoelectrochemical and dye-sensitized solar cells as well as photodetectors. The latter is rationalized by considering the transparency and conductivity of graphene, which makes it a sustainable component for electrode materials, while incorporation of electron donors is a meaningful means to tune the optical and electrical properties of graphene. Briefly, the active role of graphene in hybrids with TMCs relies on the separation of charge carriers and the minimization of charge-recombination, leading to high efficiency. However, the nature of interactions between the two species, covalent bonding vs non-covalent immobilization of TMCs onto graphene, plays a crucial role on the efficiency of electron-transfer processes within the nanoensemble. In this frame, CdSe nanoparticles were deposited onto RGO and interacted either via multiple π-π van der Waals forces or via covalent bonds. Then, when thin films of those different hybrids were fabricated, it was found that the hybrid material in which the CdSe were covalently incorporated on RGO exhibit improved quantum efficiency and photocurrent density. This example confirms the utility of the material as a novel alternative of dye/TiO_2 systems for dye sensitized solar cells. In addition, when CdTe deposited onto epitaxial graphene covered with polyethyleneglycol or polyvinylpyrrolidone, the material showed suppression of the luminescence blinking and nearly 10 times decreased luminescence intensity, as compared with bare CdTe on a glass substrate.[54]

Commercially available CdSe/ZnS dispersed in poly(methyl-methacrylate) (PMMA) matrix formed a film by spin-coating, which in turn was integrated onto CVD grown single layer graphene. The optical properties of CdSe/ZnS/graphene were examined and the photoluminescence of the material found quenched, with the emission lifetime reduced, as compared with the corresponding properties of bare CdSe/ZnS on the coverslip. The latter was attributed to the enhanced non-radiative decay that outcompetes the Auger process, leading in this way to enhanced probability of multiphonon emission.[55] Moreover, CdS and ZnS nanoparticles were *in-situ* formed onto GO via a one-step solvothermal method in which ethylene glycol served as a solvent, thiourea as the source of sulfur, while the Cd and Zn sources were the corresponding metal acetates ($M(Ac)_2$, M = Cd, Zn).[56] A significant decrease of both hybrids' photoluminescence was found, while an unexpected strong positive photovoltaic response was revealed by transient photovoltage for CdS/graphene. At the same time, separate samples of graphene and CdS nanoparticles of the same size failed to exhibit any meaningful photovoltaic response, justifying the beneficial properties of the hybrid material as contrasting its individual components.

As far as quantum dot-sensitized solar cells (QDSSCs) concern, the construction of CdS QDSSCs based on graphene-TiO_2 film photoanode and polysulfide electrolyte was accomplished.[57] Higher power conversion efficiency of 1.44 % was reported for the CdS-based QDSSC when incorporating graphene in the TiO_2 photoanode as compared to that without

graphene. The successive ionic layer adsorption was employed for the CdS deposition on the graphene-TiO_2 films, in which a two-step dipping procedure in ethanol and methanol solution was repeated for several times. Afterwards, the CdS-based QDSSCs were sealed in a sandwich structure. The improvement in the performance of the ensemble was attributed to the increased CdS adsorption, the reduction of electron recombination and the back transport reaction as well as to the enhancement of electron transport due to the presence of graphene. Alternatively, Cu_2S/RGO hybrids for high-efficiency quantum dot solar cells via a disproportionation reaction of Cu^+ (via copper(I) acetate) as a means to prepare Cu^0 nanoparticles on RGO sheets were developed.[58] Interestingly, the transportation of the electrons via the RGO sheets and the polysulfide active Cu_2S was more efficient than that on Pt electrode, improving significantly the fill factor. In addition, a sandwich CdSe quantum dot sensitized solar cell was developed by using the optimized Cu_2S/RGO composite counter electrode, which exhibited a high power conversion efficiency of 4.4 %, the highest reported so far for TMC/graphene hybrids (Scheme 6).

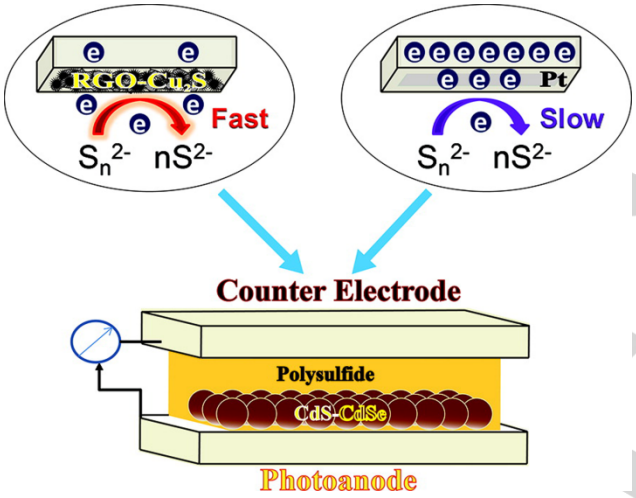

Scheme 6. Illustrative depiction of QDSSC employing Cu_2S/RGO as a counter electrode. Reprinted with permission from Ref. 58. Copyright 2011 American Chemical Society.

On a similar study, CdSe/graphene ensembles were prepared via a chemical bath deposition method that allowed to make films at low temperature for the assembly of QDSSC in the absence of a traditional wide band gap semiconductor, targeting energy conversion devices.[59] Based on TEM imaging and photoluminescence spectroscopy, it was revealed that increasing the amount of graphene the aggregation of CdSe is prevented and charge-recombination is inhibited. Notably, the application of low temperature during the fabrication process was found to be beneficial for the preparation of flexible solar cells, while the weight ratio of CdSe to GO was optimized at 4.5 and it was found that short-circuit photocurrent density and energy conversion efficiency was increased for the QDSSCs as compared with QDSSCs based on analogues of C_{60} or carbon nanotube

In 2012, the Kamat team demonstrated remarkable results when fabricated CdSe with GO, in which electron transfer from CdSe to GO was observed upon photoexcitation.[60] It was suggested that the relative rates of electron and energy transfer from the semiconducting CdSe to GO are reduced after prolonged light irradiation. The CdSe/RGO ensembles were formed by simple mixing colloidal dispersions of the two components (i.e graphene and CdSe) upon sonication. Additionally, charge separation and electron conduction were enhanced, with the presence of GO in colloidal CdSe films deposited on conducting glass electrodes enabling in that way three-dimensional sensitization. Moreover, the photoanodes that were assembled from CdSe/GO in QDSSCs displayed an enhanced photocurrent response compared to those that were prepared without GO (Scheme 7). Similarly, a flexible photoelectrode was fabricated by loading graphene sheets modified with CdSe.[61] The aforementioned ensembles showed higher efficiency and incident-photon-to-current conversion efficiency as compared to individual intact graphene and quantum dots. Moreover, based on electron transfer rate and lifetime measurements, the CdSe/graphene ensemble can be employed as active layer in photovoltaic cells since it was proved to be superior compared to intact graphene or bare CdSe.

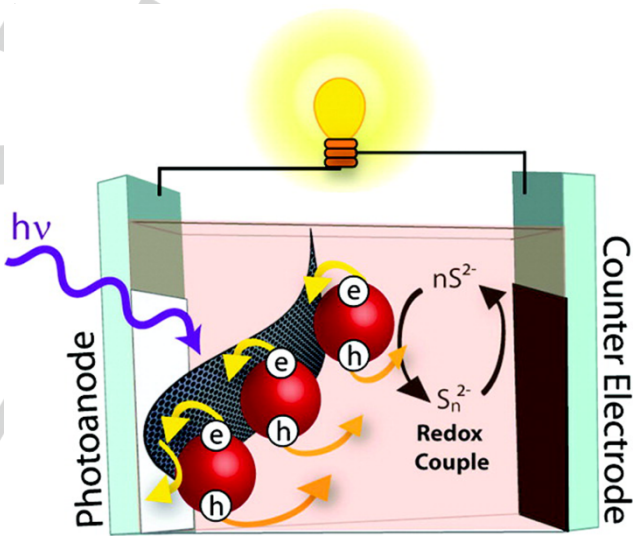

Scheme 7. Schematic illustration of QDSSCs consisting of CdSe/RGO ensembles based photoanodes. Reprinted with permission from Ref. 60. Copyright 2012 American Chemical Society.

Moreover, a sandwich structured hBN/graphene/WS_2/graphene/hBN (i.e. hBN stands for hexagonal boron nitride) photoactive device was fabricated, by using a “dry transfer” technique, which enabled the deposition of sequential flakes on top of another by annealing at each stage to prevent contamination between the layers.[62] Additionally, the van Hove singularities in the electronic density of states of TMCs enhanced light-matter interactions, hence, induced the photon absorption and the electron-hole creation. Notably, these transparent graphene electrodes led to the fabrication of extremely efficient, flexible photovoltaic devices, showing photoresponsivity above 0.1 A/W. In the same context, the fluorescence emission from individual CdSe/ZnS nanocrystals in contact with single- and few-layer graphene was tested aiming in the construction of photovoltaic devices.[63] To this end, when

CdSe/ZnS core/shell nanocrystals were spin-coated onto the graphene sheets, strong quenching of the nanocrystal fluorescence emission was achieved. For single-layer graphene sheets, the rate of energy transfer was found around 4 ns^{-1}, which is in agreement with a model based on the dipole approximation and a tight-binding description of graphene, while by increasing the number of graphene layers the rate of energy transfer was found drastically increased.

Furthermore, a different approach for the preparation of CdSe/graphene ensembles via a three-step fabrication process, namely, nanobelt deposition, graphene transfer and Ag paste, was introduced.[64] This process allows constructing Schottky junction solar cells and includes the deposition of the piece of graphene film floating on water surface laid down on one end of the CdSe nanobelt, covering the one third of the surface, after the transfer of the latter from the growth substrate onto a glass slide. Finally Ag paste was applied to the other end of the nanobelt as the negative electrode. In addition, the synthesis of active solar cells with different arrangements and connections from not only individual but also multiple assembled nanobelts was accomplished. Flexible CdSe/graphene nanobelt solar cells were reported to create diverse device architectures that can be used in cell integration placed on assembled nanobelt arrays and patterned graphene films. Finally, front electrodes for CdTe solar cells were constructed via a low-cost ambient pressure CVD procedure on graphene films, reaching a significantly high efficiency of 4.17 %.[65] Interestingly, the number of graphene layers can be controlled by the hydrogen flow rate, while the graphene films showed high mobility and transparency from 97% from one-layer films to 84% seven-layer films in the range of 350-2200 nm, rendering these conductive hybrids as new low-cost back electrodes for future photovoltaic devices.

On a slightly different theme, TMCs/graphene hybrid materials exhibit promising perspective as photodetectors. Specifically, a graphene-on-MoS_2 heterostructure photodetector was developed, where a MoS_2 monolayer was stacked on graphene by using a poly(methyl methacrylate) film as a transfer supporting layer.[66] The MoS_2 monolayer was employed to absorb light and produce electron-hole pairs, exhibited high photogain and photoresponsivity. Briefly, the structure of the hybrid enables the use of the whole surface area as a junction, where electron-hole pairs can be separated at the interface, hence, highlighting the significance of charge movement in the emerging field of 2D heterostructures.

Another challenge that the scientific community is called to confront by synthesizing more efficient and low-cost materials than the ones employed nowadays is the energy storage. Although this review focuses on light driven applications some characteristic examples on lithium ion batteries are discussed below. In this context, MoS_2/graphene hybrids prepared via an *in-situ* solution-phase method for growing MoS_2 layers on a graphene nanosheet found to exhibit great capacity and superior rate capability as well as cycling stability as anode materials for lithium ion batteries.[67] Interestingly, the highest specific capacity was achieved by the development of the aforementioned hybrid as an anode material. In addition, layered MoS_2/graphene ensembles were synthesized via an L-cys-assisted solution-phase method with sodium molybdate, as-prepared GO and L-cys as starting materials, followed by the annealing of the as-prepared MoS_2/graphene in H_2/N_2 atmosphere for the final hybrid.[68] Specifically, the three dimensional MoS_2/graphene materials exhibited excellent electrochemical performances as anode materials for Li-ion batteries. These excellent electrochemical performances of MoS_2/graphene as Li-ion battery anodes are credited to their structure and the collaborating effects between layered MoS_2 and graphene.

Significant results have also been presented by various attempts of innovative TMCs/graphene ensembles when examined in optoelectronic devices. A novel MoS_2/graphene was prepared, where MoS_2 served as the channel material and graphene was employed as both the ohmic and gate contacts and the interconnects for the 2D electronic system.[69] Both graphene and MoS_2 monolayers were synthesized by low-cost CVD methods in such way that the foundations were set for a scalable all-2D-material electronics platform that could fully exploit the mechanical flexibility and the electrostatic integrity that monolayer electronic materials offer for applications in flexible and transparent electronics. On the other hand, MoS_2/graphene binary structures that displayed remarkable dual optoelectronic functionality were fabricated by laying a graphene sheet on a MoS_2 flake at high temperature with the aid of a polymer that was later removed.[70] Specifically, the responsivity of the hybrids was nearly 1 x 10^{10} AW^{-1} at 130 K and 5 x 10^{8} AW^{-1} at room temperature, making them the most sensitive graphene-based photodetectors. Furthermore, the abovementioned hybrids can also perform as a rewritable electronic switch or memory exhibiting near perfect charge retention. These effects are ascribed to the gate-tunable charge exchange between the graphene and MoS_2 layers and may lead to new graphene-based optoelectronic devices that could be mostly used for large-area applications at room temperature. Similarly, a graphene/hBN/WS_2 sandwich structured device was developed with the “dry transfer” technique to assemble micromechanical exfoliated individual flakes for flexible and transparent electronics.[71] It was shown that a major improvement can be achieved in the device characteristics by utilizing both the tunneling and thermionic over-barrier currents in a WS_2-based field-effect tunneling transistor (FETT) to such an extent the requirements for next-generation electronic devices will be satisfied.

By employing GO in one-step aqueous hydrothermal method, CdTe/graphene were prepared, in which the growth of CdTe nanoparticles and the reduction of GO occurred simultaneously.[72] The hybrids that were composed by using the aforementioned environmental-friendly and time saving approach, demonstrated enhanced photoresponses, rendering them suitable for optoelectronics applications. Furthermore, photoresponse measurements revealed that the CdTe/graphene electrode exhibited higher photovoltage and photocurrent performance than CdTe nanoparticles themselves.

In 2012, the Guldi team developed a well-designed hybrid material composed from CdTe and exfoliated graphene rather than GO and/or RGO in aqueous media.[19] This was accomplished by employing two different approaches. In brief, according to the first approach pyrene-functionalized CdTe nanoparticles were interacted with exfoliated graphene via hydrophobic π-π stacking interactions, whereas on the second approach, graphene was non-covalently functionalized with a positively charged pyrene derivative which then electrostatically coupled with negatively charged CdTe nanoparticles, according to Scheme 8. Following these methods, the rough oxidation steps to prepare graphene oxide and the subsequent chemical

reduction to reduced graphene oxide were avoided, while the basic properties of graphene were retained. Both CdTe-pyrene/graphene and CdTe/pyrene$^+$/graphene ensembles support electron transfer dynamics. However, the exfoliation degree of graphene is essential since the higher it is the better charge-transfer properties are accomplished.

Table 2 summarizes the photovoltaic performance parameters for the reviewed TMC/graphene ensembles. In brief, the RGO/CdS-CdSe[58] along with the graphene/ZnO/CdS/CdTe[65] as photoanode electrodes exhibit high energy conversion efficiency (η) values of 4.4 and 4.17% respectively, as well as high short circuit photocurrent density (J_{sc}) of 18.4 and 22.9 mA cm^{-2}, respectively. It should be mentioned that for the former system, RGO/Cu_2S was used as a counter photocathode electrode, while for the latter graphene, both contrasting the widely applied Pt or Au as counter electrodes. The enhanced absorption owed to the combination of two quantum dots in the form of CdS/CdTe[58, 65] is beneficial for obtaining superior photovoltaic performance, as compared to the case where the single quantum dot CdSe[57, 59, 61, 64] was tested. Markedly, the presence of graphene either as stand-alone material or in conjunction with CuS_2 nanoparticles, playing the role of the counter photocathode electrode, is advantageous as compared with the widely employed Pt or Au on FTO/ITO. The latter is further realized by examining the fill factor (FF) value, which is the highest (0.46) among the materials currently reviewed. On the other hand, the highest open circuit voltage (V_{oc}) value was registered for graphene/CdS, employing Au-FTO as counter photocathode electrode, however in combination with the rest photovoltaic parameters, its energy conversion efficiency was found only at 1.44%.[57] By extension, future research on synthesizing advanced graphene-based ensembles, in which binary and ternary TMCs with well-designed structure (i.e. alloyed, core-shell) are integrated onto graphene, is expected to further advance the field aiming improved photovoltaic performances.

Table 2. Photovoltaic parameters for TMC/graphene ensembles employed as photoanode electrodes.

Photoanode Electrode	Counter Photocathode Electrode	η %	FF	V_{oc}/V	J_{sc}/mA cm^{-2}	Ref.
Graphene/CdS	Au-FTO	1.44	0.35	0.58	7.1	57
RGO/CdS-CdSe	RGO-Cu_2S	4.4	0.46	0.52	18.4	58
Graphene/CdSe	Pt-FTO	0.76	0.37	0.35	5.8	59
Graphene/CdSe	Pt-ITO	0.58	0.42	0.52	2.6	61
Graphene/CdSe	CNT	0.11	0.24	0.49	0.94	64
Graphene/ZnO/CdS/CdTe	Graphene	4.17	0.42	0.43	22.9	65

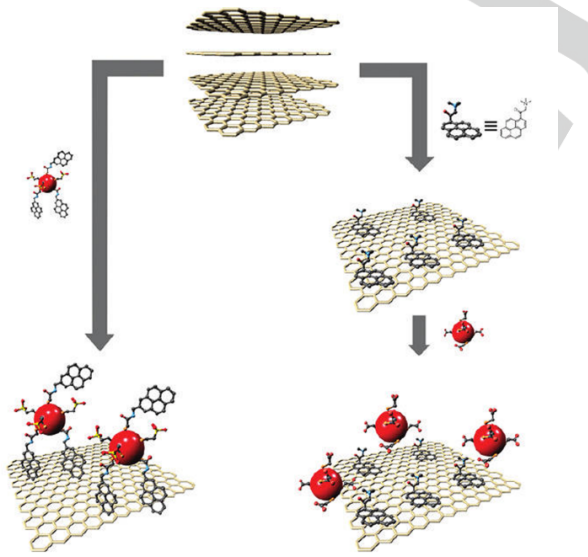

Scheme 8. Illustration of CdTe-pyrene/graphene and CdTe/pyrene$^+$/graphene ensembles formed by π-π stacking interactions between exfoliated graphene and pyrene moieties. Reprinted with permission from Ref. 19. Copyright 2012 American Chemical Society.

4. TMCs/Graphene Ensembles for Biosensing

Functional TMC/graphene ensembles can be also employed in biosensing applications. In this framework, CuS/graphene with well-defined morphology was successfully fabricated via the conventional *in-situ* hydrothermal route by employing thioacetamide as both the sulfur source and the reducing agent (Scheme 9).[73] The ensembles exhibited a higher peroxidase-like catalytic activity than bare CuS in acetate buffer solution, attributed to the dispersibility preference and the maximum synergistic interaction between graphene and CuS nanoflakes. Furthermore, the CuS/graphene ensemble can be used as an artificial enzyme in biosensors and environmental monitoring of H_2O_2.

In addition, CdSe was successfully attached to oxidized graphene-(*p*-phenylenediamine) nanosheets through the formation of CdSe and their spontaneous self-assembly on *p*-phenylenediamine reduced graphene nanosheets.[74] The hybrids demonstrated different fluorescent activities than those exhibited so far due to the blocking role of the long chain alkane surfactant molecules between the graphene and the CdSe nanoparticles, rendering them potential candidates for bio-imaging applications and light emitting devices. In addition, poly(diallyl-dimethylammonium chloride) (PDDA) – functionalized graphene

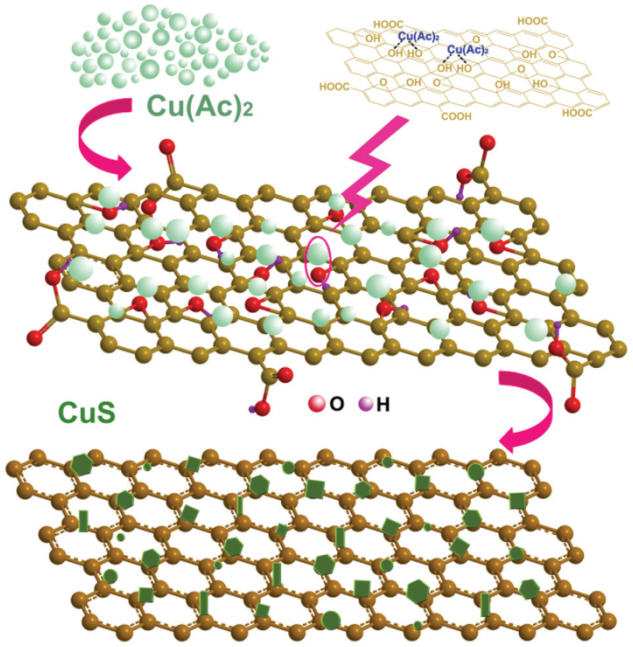

Scheme 9. Illustration showing the preparation route of CuS/graphene ensemble employed as biosensor. Reproduced from Ref. 73 with permission of The Royal Society of Chemistry.

(CdTe/PDDA-graphene), decorated with CdTe nanoparticles, was synthesized via a simple one-step chemical reduction of exfoliated GO in the presence of PDDA and CdTe. The material was found highly selective to puerarin (7,4-dihydroxyisoflavone-8-glucopyranoside), which is a major active ingredient in the traditional Chinese medicine.[75] The ultrafast electron transfer property combined with the absorption selectivity towards puerarin, contributed to fabricate a puerarin sensor with superior electrochemical activity.

On a different application, a CdS/GO photoelectrochemical biosensor was realized to detect the carcinoembryonic antigen. The novelty of the system deals with the preparation of CdS nanoparticles onto GO as catalyzed upon the reduction of sodium thiosulfate by hydrogen peroxide detected on the horseradish peroxidase.[76] Notably, it was shown that enzymes can be employed in the deposition of inorganic nanoparticles onto graphene sheets.

5. Conclusions and Prospects

Combining TMCs based on VIA, IB and IIB metals of the periodic table with graphene sheets yields TMCs/graphene hybrid materials that exhibit excellent photocatalytic properties suitable for hydrogen evolution, degradation of organic pollutants and redox reactions, as well as with high prospect to be employed in photovoltaic devices, photodetectors and biosensing. The *in-situ* formation and growth of TMCs onto graphene is a method that was extensively used for the fabrication of such TMCs/graphene ensembles, whereas other routes include electrostatic interactions, simple mixing, while also deposition of TMCs onto graphene substrates is applied when electronic devices are concerned. Employment of TMCs for solar harvesting application carries several benefits over the conventionally used TiO_2, since TMCs are photostable and high surface area visible light absorbers. Markedly, incorporation of TMCs on graphene in energy applications is significant, for inhibiting charge recombination processes, increasing the specific surface area and creating more catalytic active sites. Notably, in many cases TMC/graphene ensembles outclass the most conventional utilized material for a particular purpose by demonstrating improved photocatalytic performances and increased photoresponse behaviour.

The majority of the abovementioned utilities of graphene/TMCs are still considered as basic research, suggesting that there are still many steps to climb until commercial products for everyday life will be realized. Although fabrication methods have yet to be optimized, the prospect is high, particularly when considering the exceptional performances demonstrated in a large range of applications. However in most cases, GO or RGO have been employed as supporting material for TMCs, when defect-free exfoliated graphene carries higher potentiality due to its improved electronic and ballistic charge transport properties. Therefore, additional effort is certainly required to take full benefit of the novel characteristics of graphene that may lead to better functional materials. We believe that this review will inspire and encourage researchers to make new and significant contributions in this fascinating and rapidly evolving field.

Acknowledgements

This project has received funding from the European Union's Horizon 2020 research and innovation programme under the Marie Sklodowska-Curie grant agreement No 642742. Partial financial support by the General Secretariat for Research and Technology, Greece, through project "Advanced Materials and Devices" (MIS: 5002409) is acknowledged.

Keywords: graphene • transition metal chalcogenides • hybrids • functional materials • energy conversion

[1] M.-R. Gao, Y.-F. Xu, J. Jiang and S.-H. Yu, *Chem. Soc. Rev.* **2013**, *42*, 2986-3017.
[2] J. Park, J. Joo, S. G. Kwon, Y. Jang and T. Hyeon, *Angew. Chem., Int. Ed.* **2007**, *46*, 4630-4660.
[3] M. A. Malik, P. O'Brien and N. Revaprasadu, *Chem. Mater.* **2002**, *14*, 2004-2010.
[4] P. K. Santra and P. V. Kamat, *J. Am. Chem. Soc.* **2013**, *135*, 877-885.
[5] H. Zhong, Y. Zhou, M. Ye, Y. He, J. Ye, C. He, C. Yang and Y. Li, *Chem. Mater.* **2008**, *20*, 6434-6443.
[6] K. Meng, G. Chen and K. R. Thampi, *J. Mater. Chem. A* **2015**, *3*, 23074-23089.
[7] X. Chia, A. Ambrosi, D. Sedmidubský, Z. Sofer and M. Pumera, *Chem. Eur. J.* **2014**, *20*, 17426-17432.
[8] L. Wang, Z. Sofer, J. Luxa and M. Pumera, *Adv. Mater. Interfaces* **2015**, *2*.
[9] P. V. Kamat, *Acc. Chem. Res.* **2012**, *45*, 1906-1915.
[10] A. Ye, W. Fan, Q. Zhang, W. Deng and Y. Wang, *Catal. Sci. Technol.* **2012**, *2*, 969-978.
[11] Y. Liang, Y. Li, H. Wang and H. Dai, *J. Am. Chem. Soc.* **2013**, *135*, 2013-2036.
[12] Z. Yao, L. Wang, Y. Zhang, Z. Yu and Z. Jiang, *Int. J. Hydrogen Energy* **2014**, *39*, 15380-15386.
[13] B. Qu, C. Li, C. Zhu, S. Wang, X. Zhang and Y. Chen, *Nanoscale* **2016**, *8*, 16886-16893.

[14] A. H. Castro Neto, F. Guinea, N. M. R. Peres, K. S. Novoselov and A. K. Geim, *Rev. Mod. Phys.* **2009**, *81*, 109.
[15] M. S. Fuhrer, C. N. Lau and A. H. MacDonald, *MRS Bull.* **2010**, *35*, 289-295.
[16] A. K. Geim and K. S. Novoselov, *Nat. Mater.* **2007**, *6*, 183-191.
[17] X. Du, I. Skachko, A. Barker and E. Y. Andrei, *Nat. Nanotechnol.* **2008**, *3*, 491-495.
[18] K. I. Bolotin, K. Sikes, Z. Jiang, M. Klima, G. Fudenberg, J. Hone, P. Kim and H. Stormer, *Solid State Commun.* **2008**, *146*, 351-355.
[19] G. Katsukis, J. Malig, C. Schulz-Drost, S. Leubner, N. Jux and D. M. Guldi, *ACS Nano* **2012**, *6*, 1915-1924.
[20] C. Nethravathi, T. Nisha, N. Ravishankar, C. Shivakumara and M. Rajamathi, *Carbon* **2009**, *47*, 2054-2059.
[21] Y. Zhang, J. Tian, H. Li, L. Wang, X. Qin, A. M. Asiri, A. O. Al-Youbi and X. Sun, *Langmuir* **2012**, *28*, 12893-12900.
[22] F. Meng, J. Li, S. K. Cushing, M. Zhi and N. Wu, *J. Am. Chem. Soc.* **2013**, *135*, 10286-10289.
[23] P. V. Kamat, *J. Phys. Chem. C* **2007**, *111*, 2834-2860.
[24] X. Xie, K. Kretschmer and G. Wang, *Nanoscale* **2015**, *7*, 13278-13292.
[25] M. G. Walter, E. L. Warren, J. R. McKone, S. W. Boettcher, Q. Mi, E. A. Santori and N. S. Lewis, *Chem. Rev.* **2010**, *110*, 6446-6473.
[26] K. Zeng and D. Zhang, *Prog. Energy Combust. Sci.* **2010**, *36*, 307-326.
[27] J. Zhang, J. Yu, M. Jaroniec and J. R. Gong, *Nano Lett.* **2012**, *12*, 4584-4589.
[28] Q. Li, H. Meng, J. Yu, W. Xiao, Y. Zheng and J. Wang, *Chem. Eur. J.* **2014**, *20*, 1176-1185.
[29] W.-J. Ong, J.-J. Yeong, L.-L. Tan, B. T. Goh, S.-T. Yong and S.-P. Chai, *RSC Adv.* **2014**, *4*, 59676-59685.
[30] Q. Li, B. Guo, J. Yu, J. Ran, B. Zhang, H. Yan and J. R. Gong, *J. Am. Chem. Soc.* **2011**, *133*, 10878-10884.
[31] X.-J. Lv, W.-F. Fu, H.-X. Chang, H. Zhang, J.-S. Cheng, G.-J. Zhang, Y. Song, C.-Y. Hu and J.-H. Li, *J. Mater. Chem.* **2012**, *22*, 1539-1546.
[32] L. Jia, D.-H. Wang, Y.-X. Huang, A.-W. Xu and H.-Q. Yu, *J. Phys. Chem. C* **2011**, *115*, 11466-11473.
[33] F.-X. Xiao, J. Miao and B. Liu, *J. Am. Chem. Soc.* **2014**, *136*, 1559-1569.
[34] T. Skaltsas, N. Karousis, S. Pispas and N. Tagmatarchis, *Nanotechnology* **2014**, *25*, 445404.
[35] B. Zhu, B. Lin, Y. Zhou, P. Sun, Q. Yao, Y. Chen and B. Gao, *J. Mater. Chem. A* **2014**, *2*, 3819-3827.
[36] Y. Li, H. Wang, L. Xie, Y. Liang, G. Hong and H. Dai, *J. Am. Chem. Soc.* **2011**, *133*, 7296-7299.
[37] Q. Xiang, J. Yu and M. Jaroniec, *J. Am. Chem. Soc.* **2012**, *134*, 6575-6578.
[38] H. Tang, K. Dou, C.-C. Kaun, Q. Kuang and S. Yang, *J. Mater. Chem. A* **2014**, *2*, 360-364.
[39] I. K. Konstantinou and T. A. Albanis, *Appl. Catal., B* **2004**, *49*, 1-14.
[40] A. Houas, H. Lachheb, M. Ksibi, E. Elaloui, C. Guillard and J.-M. Herrmann, *Appl. Catal., B* **2001**, *31*, 145-157.
[41] H. Lachheb, E. Puzenat, A. Houas, M. Ksibi, E. Elaloui, C. Guillard and J.-M. Herrmann, *Appl. Catal., B* **2002**, *39*, 75-90.
[42] S. Sakthivel, B. Neppolian, M. V. Shankar, B. Arabindoo, M. Palanichamy and V. Murugesan, *Sol. Energy Mater. Sol. Cells* **2003**, *77*, 65-82.
[43] S. K. Kansal, M. Singh and D. Sud, *J. Hazard. Mater.* **2007**, *141*, 581-590.
[44] H. Zhu, R. Jiang, L. Xiao, Y. Chang, Y. Guan, X. Li and G. Zeng, *J. Hazard. Mater.* **2009**, *169*, 933-940.
[45] J. Yu, J. Zhang and S. Liu, *J. Phys. Chem. C* **2010**, *114*, 13642-13649.
[46] Z. Gao, N. Liu, D. Wu, W. Tao, F. Xu and K. Jiang, *Appl. Surf. Sci.* **2012**, *258*, 2473-2478.
[47] J. Shi, X. Zhou, Y. Liu, Q. Su, J. Zhang and G. Du, *Mater. Lett.* **2014**, *126*, 220-223.
[48] P. Chen, T.-Y. Xiao, H.-H. Li, J.-J. Yang, Z. Wang, H.-B. Yao and S.-H. Yu, *ACS Nano* **2012**, *6*, 712-719.
[49] M.-Q. Yang, C. Han, N. Zhang and Y.-J. Xu, *Nanoscale* **2015**.
[50] Y. Zhang, N. Zhang, Z.-R. Tang and Y.-J. Xu, *ACS Nano* **2012**, *6*, 9777-9789.
[51] N. Zhang, Y. Zhang, X. Pan, X. Fu, S. Liu and Y.-J. Xu, *J. Phys. Chem. C* **2011**, *115*, 23501-23511.
[52] N. Zhang, Y. Zhang, X. Pan, M.-Q. Yang and Y.-J. Xu, *J. Phys. Chem. C* **2012**, *116*, 18023-18031.
[53] X. Liu, L. Pan, T. Lv, G. Zhu, Z. Sun and C. Sun, *Chem. Commun.* **2011**, *47*, 11984-11986.
[54] T. Hirose, Y. Kutsuma, A. Kurita, T. Kaneko and N. Tamai, *Appl. Phys. Lett.* **2014**, *105*, 083102.
[55] J. Liu, P. Kumar, Y. Hu, G. J. Cheng and J. Irudayaraj, *J. Phys. Chem. C* **2015**, *119*, 6331-6336.
[56] P. Wang, T. Jiang, C. Zhu, Y. Zhai, D. Wang and S. Dong, *Nano Res.* **2010**, *3*, 794-799.
[57] G. Zhu, T. Xu, T. Lv, L. Pan, Q. Zhao and Z. Sun, *J. Electroanal. Chem.* **2011**, *650*, 248-251.
[58] J. G. Radich, R. Dwyer and P. V. Kamat, *J. Phys. Chem. Lett.* **2011**, *2*, 2453-2460.
[59] S. Sun, L. Gao, Y. Liu and J. Sun, *Appl. Phys. Lett.* **2011**, *98*, 093112.
[60] I. V. Lightcap and P. V. Kamat, *J. Am. Chem. Soc.* **2012**, *134*, 7109-7116.
[61] J. Chen, F. Xu, J. Wu, K. Qasim, Y. Zhou, W. Lei, L.-T. Sun and Y. Zhang, *Nanoscale* **2012**, *4*, 441-443.
[62] L. Britnell, R. M. Ribeiro, A. Eckmann, R. Jalil, B. D. Belle, A. Mishchenko, Y.-J. Kim, R. V. Gorbachev, T. Georgiou, S. V. Morozov, A. N. Grigorenko, A. K. Geim, C. Casiraghi, A. H. C. Neto and K. S. Novoselov, *Science* **2013**, *340*, 1311-1314.
[63] Z. Chen, S. Berciaud, C. Nuckolls, T. F. Heinz and L. E. Brus, *ACS Nano* **2010**, *4*, 2964-2968.
[64] L. Zhang, L. Fan, Z. Li, E. Shi, X. Li, H. Li, C. Ji, Y. Jia, J. Wei and K. Wang, *Nano Res.* **2011**, *4*, 891-900.
[65] H. Bi, F. Huang, J. Liang, X. Xie and M. Jiang, *Adv. Mater.* **2011**, *23*, 3202-3206.
[66] W. Zhang, C.-P. Chuu, J.-K. Huang, C.-H. Chen, M.-L. Tsai, Y.-H. Chang, C.-T. Liang, Y.-Z. Chen, Y.-L. Chueh, J.-H. He, M.-Y. Chou and L.-J. Li, *Sci. Rep.* **2014**, *4*, 3826.
[67] K. Chang and W. Chen, *Chem. Commun.* **2011**, *47*, 4252-4254.
[68] K. Chang and W. Chen, *ACS Nano* **2011**, *5*, 4720-4728.
[69] L. Yu, Y.-H. Lee, X. Ling, E. J. G. Santos, Y. C. Shin, Y. Lin, M. Dubey, E. Kaxiras, J. Kong, H. Wang and T. Palacios, *Nano Lett.* **2014**, *14*, 3055-3063.
[70] K. Roy, M. Padmanabhan, S. Goswami, T. P. Sai, G. Ramalingam, S. Raghavan and A. Ghosh, *Nat. Nanotechnol.* **2013**, *8*, 826-830.
[71] T. Georgiou, R. Jalil, B. D. Belle, L. Britnell, R. V. Gorbachev, S. V. Morozov, Y.-J. Kim, A. Gholinia, S. J. Haigh, O. Makarovsky, L. Eaves, L. A. Ponomarenko, A. K. Geim, K. S. Novoselov and A. Mishchenko, *Nat. Nanotechnol.* **2013**, *8*, 100-103.
[72] Z. Lu, C. X. Guo, H. B. Yang, Y. Qiao, J. Guo and C. M. Li, *J. Colloid Interface Sci.* **2011**, *353*, 588-592.
[73] G. Nie, L. Zhang, X. Lu, X. Bian, W. Sun and C. Wang, *Dalton Trans.* **2013**, *42*, 14006-14013.
[74] Y. Wang, H.-B. Yao, X.-H. Wang and S.-H. Yu, *J. Mater. Chem.* **2011**, *21*, 562-566.
[75] R. Yang, D. Miao, Y. Liang, L. Qu, J. Li and P. d. B. Harrington, *Electrochim. Acta* **2015**, *173*, 839-846.
[76] X. Zeng, W. Tu, J. Li, J. Bao and Z. Dai, *ACS Appl. Mater. Interfaces* **2014**, *6*, 16197-16203.

REVIEW

Transition metal chalcogenides/graphene ensembles are a novel class of materials for energy applications particularly in photocatalysis, photovoltaics and biosensing. In this Review, we critically present and evaluate the development in the field by demonstrating key-examples from the recent literature.

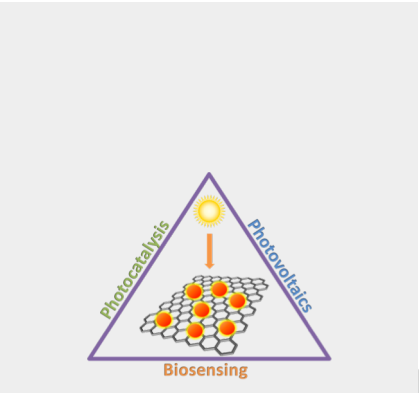

*Antonia Kagkoura, Theodosis Skaltsas and Nikos Tagmatarchis**

Page No. – Page No.

Transition metal chalcogenides/graphene ensembles for light-induced energy applications